文章编号:2095-0411(2017)03-0006-07

Characterization of Ferroelectric-Ferromagnetic Multilayered Nanocomposite Films Using a Modified Sol-Gel Process

WANG Mengying[1], YUAN Jia[1], HOU Fang[1], JIANG Yulin[1], ZHANG Hongfang[1], KARAKI Tomoaki[2]
(1. Department of Physics, Suzhou University of Science and Technology, Suzhou 215009, China; 2. Toyama Prefectural University, Imizu, Toyama 939-0398, Japan)

Abstract: Polymer-assistant polyvinylpyrrolidone (PVP-K30) was introduced to the sol-gel processing route, and multilayered nanocomposite films of $Pb(Zr_{0.52}Ti_{0.48})O_3$-$(Ni_{0.5}Zn_{0.5})Fe_2O_4$ (PZT-NZFO) were fabricated on $Pt/Ti/SiO_2/Si$ substrates successfully by spin-coating at low firing temperatures 600℃. Structural characterization by X-ray diffraction and electron microscopy techniques reveals good surface and well-controlled cross-sectional morphologies of these films. Coexistence of ferromagnetic and ferroelectric phases with obvious ferromagnetic and ferroelectric hysteresis loops are observed at room temperature. An appropriate dielectric constant with low loss tangent is obtained in low frequency exhibiting excellent dielectric properties. The dielectric properties of nanocomposite thin film shows at 1kHz and room temperature, the dielectric constant and loss tangent for the nanocomposite films are about 165 and 0.02. While the room-temperature magnetization values (M_s) is about 2.6×10^4 A/m, and the intrinsic coercivity (H_{ci}) is about 1.19×10^4 A/m, respectively. The combination of high permeability and permittivity in the nanocomposite films presents potential applications in of the fields of microelectronic devices and integrated units.

Key words: nanocomposites; polymer-assistance; sol-gel process; ferroelectric hysteresis; ferromagnetic hysteresis
中图分类号:TB 3 **文献标志码**:A **doi**:10.3969/j.issn.2095-0411.2017.03.002

优化的溶胶-凝胶法制备多层铁电-铁磁纳米复合薄膜

王梦影[1],袁 佳[1],侯 芳[1],姜玉琳[1],张红芳[1],唐木智明[2]
(1. 苏州科技大学 数理学院,江苏 苏州 215009;2. 日本富山县大学,射水 富山 939-0398)

摘要: 在溶胶-凝胶的前驱体中加入高聚物聚乙烯吡咯烷酮(PVP-K30),可以在烧结温度 600℃成功制备沉积在 $Pt/Ti/SiO_2/Si$ 基片上多层结构的 $Pb(Zr_{0.52}Ti_{0.48})O_3$-$Ni_{0.5}Zn_{0.5}Fe_2O_4$(PZT-NZFO)纳米复合薄膜。采用 X-ray 衍射仪测定纳米薄膜的相结构,扫描电镜与原子力显微镜观察纳米复合薄膜的表面形貌。相结构分析表明:铁电相与铁磁相共存在 PZT-NZFO 纳米复合薄膜中;微观形貌表明:表面微观形貌致密,无裂纹;此外,PZT-NZFO 中 PZT 层与 NZFO 层相互交替,并且层与层之间的厚度可以得到较好地控制。PZT-NZFO 纳米复合薄膜呈现明显

收稿日期:2016-11-10。
基金项目:江苏省自然科学基金资助项目(BK20131153,BK20140278)。
作者简介:王梦影(1995—),女,江苏海安人。通讯联系人:张红芳(1968—),女,江苏丹阳人,博士,副教授,主要从事功能材料与复合材料的研究。E-mail: constance_zhanghf@126.com

的电滞回线与磁滞回线，进一步证明了 PZT-NZFO 复合纳米薄膜中同时存在着铁电相与铁磁相。介电性能显示：室温在 1kHz，相对介电常数和介电损耗分别为 165 和 0.02。磁性能结果显示：室温时，PZT-NZFO 纳米复合薄膜的饱和磁化强度为 2.6×10^4 A/m，内在矫顽力为 1.19×10^4 A/m。加入高聚物后改进的溶胶-凝胶制备的 PZT-NZFO 复合纳米薄膜实验结果表明，这种致密的、无裂纹的、介电损耗低，并同时具有铁电与磁电的纳米复合薄膜在微型器件与集成电路中具有潜在的应用。

关键词：纳米复合物；高聚物辅助；溶胶-凝胶；磁滞回线；电滞回线

Ferroelectric-ferromagnetic materials are particularly appealing because they have the properties of both parent compounds, but also because interactions between the magnetic and electric polarizations lead to their multifunctionality[1]. Moreover, they have high dielectric permittivity and magnetic permeability, and could therefore replace the inductor and capacitor in resonant circuits with a single component, further miniaturizing portable cellular technologies[2]. Recently, the Ferroelectric-ferromagnetic composite materials were found that elastic deformation is potential applications in actuators, transducers, field sensor and data storage devices[3-6]. Importantly, motivated by on-chip integration in microelectronic devices, nanostructured composites of ferroelectric and magnetic composites have recently been deposited in a film-on substrate geometry[7-10], however, the availability of high-quality nanostructured composites is premium importance, which makes it easier to tailor their properties, offering a technical way to study the physical mechanism in nano-scale and potential applications in microelectronic devices[11]. Additionally, as for integrated circuit in the case of silicon substrates, it would be better to maintain the firing temperature of the films lower than 750℃ in order to avoid apparent chemical reactions between the film and the silicon substrate. Unfortunately the multilayer multiferroic thin films reported in the literatures was fired at least or over 750℃ by solution processing, which is absolutely strict to the films application furthermore[5,7].

The objective of the present work is to fabricate multilayered structured nanocomposites films of Pb($Zr_{0.52}Ti_{0.48}$)O_3(PZT) and ($Ni_{0.5}Zn_{0.5}$)Fe_2O_4(NZFO) on Pt/Ti/SiO_2/Si substrates via a sol-gel process modified by polymer-assistant polyvinylpyrrolidone cofiring at low temperature annealing of 600℃. Piezoelectric PZT ceramics having the composition at the morphotropic phase boundary ($x=0.52$) normally have a higher permittivity, larger losses and much higher piezoelectric coupling. And inverse spinel nickel ferrite NZFO has good magnetostrictive properties which are dependent on composition and preparation method[12]. Due to its properties, this system (($Ni_{0.5}Zn_{0.5}$)Fe_2O_4) was often used as magnetic component in magnetoelectric composites[13-14]. and also chosen in this work to form ferroelectric and ferromagnetic nanocomposite thin films.

We have achieved levels of the crystalline phase that are higher than any previously reported with a dense, crack-free microstructure of a nano-scale multilayered structured films with a thickness of about 1μm . The processing route, crystallization behavior and microstructures, dielectric properties, magnetic properties and ferroelectricity are investigated in detail in the following sections.

1 Experimental

1.1 Processing route for preparing polymer-assistant sol precursor

The Pb($Zr_{0.52}Ti_{0.48}$)O_3(PZT) and ($Ni_{0.5}Zn_{0.5}$)Fe_2O_4(NZFO) sol precursor solutions were modified by polymer-assistant polyvinylpyrrolidone (PVP-K30 with number-average molecular weight of 10 000)[15-16]. PZT films were prepared from solutions of molar compositions, n(Pb($CH_3COO)_2$)∶n(Zr[$CH_3C(O)CHC(O)CH_3$]$_4$)∶n(Ti(OC_4H_9)$_4$)∶n(PVP)∶n($C_3H_7^iOH$)＝1∶0.52∶0.48∶1∶20, where moles of PVP represent those of the monomer (polymerizing repeating unit) of PVP. The procedure for

preparing the starting solutions is described as follows. PVP was firstly dissolved in $C_3H_7^iOH$ thoroughly; then, the $Ti(OC_4H_9)_4$ solution chelated by a mixture of 2-Methoxyethanol and acetylacetone was added to the PVP-$C_3H_7^iOH$ solution successively under stirring at room temperature for 30min. Commercial $Pb(CH_3COO)_2 \cdot 3H_2O$ and $Zr[CH_3C(O)CHC(O)CH_3]_4$ powders in proper molar ratio were dissolved in hot 2-Methoxyethanol. Then, the $Pb(CH_3COOH)_2$-$Zr[CH_3C(O)CHC(O)CH_3]_4$ solution was added in drop wise to the $Ti(OC_4H_9)_4$-PVP-$C_3H_7^iOH$ solution under vigorous stirring at 80℃ for 2h, the concentration of the PZT sol precursor was 0.4mol/L. A light yellowish and transparent solution was then obtained, and served as the coating solution.

Similarly, NZFO films were prepared from solutions of molar compositions, $n(Ni(CH_3COO)_2):n(Zn(CH_3COO)_2):n(Fe(NO_3)_3):n(PVP):n(C_3H_7^iOH)=0.5:0.5:2:1:20$, in this experiment, a small mount of $Ti(OC_4H_9)_4$ was employed in order that the polymer-assistant (PVP) can be introduced in the NZFO sol precursor. And the mass ratio of the $Ti(OC_4H_9)_4$ to the PVP was 0.1% to give a balance between the processing behavior and properties of the resulting thin films. PVP was firstly dissolved in $C_3H_7^iOH$, then, the $Ti(OC_4H_9)_4$ was added to the PVP-$C_3H_7^iOH$ solution thoroughly. Commercial $Ni(CH_3COO)_2 \cdot 6H_2O$, $Zn(CH_3COO)_2 \cdot 4H_2O$, and $Fe(NO_3)_3 \cdot 9H_2O$ powders were dissolved in hot 2-Methoxyethanol for 2h, then, the PVP-$C_3H_7^iOH$-$Ti(OC_4H_9)_4$ solution was added in drop wise to the $Ni(CH_3COO)_2$-$Zn(CH_3COO)_2$-$Fe(NO_3)_3$ with vigorous stirring at 50℃ for 2h. The concentration of the NZFO sol-gel precursor was 0.4mol/L. The PZT and NZFO sol precursors were sealed in glass containers at room temperature, respectively, which was ready for further processes.

1.2 Synthesis of multilayered nanocomposites thin films

The multilayered PZT/NZFO nanocomposite thin films were deposited with a simple spin-coating deposition on the Pt/Ti/SiO_2/Si substrate at 3 000r/min for 20s alternatively, and each layer of film (the pure PZT and pure NZFO thin films successively according to the designed film patterns) was preheated at 110℃, 400℃ for 5min to remove organic components. The spin coating process was repeated by coating 9 layers until desired thickness about 1 μm was reached. The resultant films were then fired at 500—600℃ for 30min at air in muffle furnace to crystallize the films. The structure of the nanocomposite films is 2PZT/CFO/2PZT/CFO/2PZT/CFO (denoted as PZT-NZFO), referring to the PZT as the first layer deposited on the substrate with double layers, subsequently, the NZFO as the second layer with one layer deposited on the preheated PZT layer alternatively.) Moreover, for comparison with the nanocomposite films, the pure PZT and NZFO thin films were also deposited on the Pt/Ti/SiO_2/Si substrate by spin-coating with the above-described PZT and NZFO sol precursors with the thickness of about 1 μm respectively.

1.3 Property Measurements

The X-ray diffraction (XRD) patterns of the films at room temperature were characterized using an X-ray diffractrometer (Philips X'Pert-Pro MPD) with CuKα1 radiation (0.154 06nm, 40kV, 30mA). Atomic force microscopy (AFM, Nanoscope IV di Digital Instruments) and a field-emission scanning electron microscope (SEM) (JEOL JSM-6335F) were used for observation of the film microstructures. Differential Scanning Calorimeter and Thermal-Gravimetric Analysis (DSC-TGA, Netzch STA 449C, Jupiter) was introduced to analyze the sol precursors (i.e. the precursor solutions of PZT & NZFO) at a heating rate of 10℃/min.

The magnetization-magnetic field in-plane hysteresis loops were measured using a vibrating sample magnetometer (VSM) (Lakeshore 7 300 series) at room temperature. The sample dimension is 10 mm×10 mm with the thickness of 1μm.

All samples were coated by a top gold (Au) electrode with a 0.5 mm×0.5 mm square for electrical performance measurements. The dielectric properties dependence on the frequency were measured with Agilent 4 294 A impedance analyzer. A TF Analyzer 2 000 (aix ACT, Co.) was employed to investigate the polarization-electric field (P-E) hysteresis loops at a frequency of 1kHz at room temperature.

2 Results and Discussion

2.1 Crystallization behavior and microstructure

Figure 1 shows the DSC and TGA plots of the PVP-containing (a) PZT and (b) NZFO precursor gel dried at 120℃ in the air, respectively. In Fig. 1(a), two exothermic peaks (DSC) were observed at round 250℃ and 475℃, respectively. The exothermic peak at 250℃ reflects the decomposition of the organic products, including polymeric PVP, carbon dioxide and nitrogen dioxide[17]. At the same time, compared with the final residual mass (%) shown in plot of TGA, a large mass loss of 28% was occurred. And the exothermic peak observed at 475℃ is the crystallization temperature of PZT precursor gel, along with the minor mass loss of 4%, and no weight loss is observed above 500℃, suggesting that PVP decomposition is completed at this temperature, when the PZT crystallization starts. Therefore, the crystalline PZT phase can be derived from the PZT film sol precursor at a low temperature annealing of 500℃.

As shown in Fig. 1(b), three exothermic peaks were observed at about 250℃, 300℃ and 430℃, respectively. Similarly, the exothermic peak of 250℃ is recognized as the decomposition PVP and combustion of bound organics, and the exothermic peak of 300℃ is attributed to thermoxidative degradation of and ferric nitrate[18], and the crystallization temperature of NZFO is occurred at 420℃ with the mass loss of 0.33%, and above 450℃, practically weight loss could not be observed any more. Hence, the annealing temperature is selected at 500℃, which is enough for the formation of spinel structure NZFO crystal phase from the NZFO sol precursor.

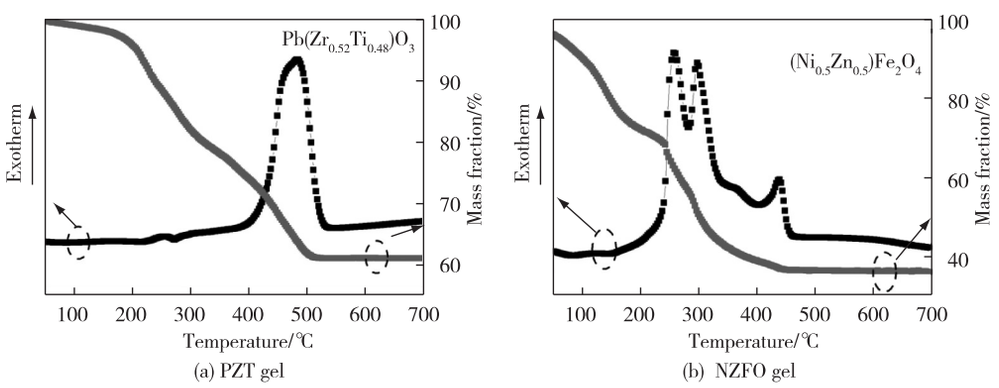

Fig.1　The DSC and TGA curves of the PVP-containing gel dried at 120 ℃, respectively

Figure 2 shows the X-ray diffraction (XRD) patterns: Fig. 2(a) pure PZT films annealing at 600℃, Fig. 2(b) pure NZFO annealing at 500℃, together with Fig. 2(c) the PZT-NZFO nanocomposite thin films annealing at 600℃. As shown in Fig. 2, the crystallization behavior observed by XRD agrees with DTA-TAG results. For example, in Fig. 2(a), all the peaks indicate the presence of pure PZT film with a perovskite structure, and in the curve of Fig. 2(b), the pure NZFO thin film is characterized as a pure, crystalline Ni-Zn ferrite with a spinel structure except for the 2 theta equal to 46°, we contribute to the introduction of the minor mount of Ti^{4+} in the NZFO precursor solution[12]. In Fig. 2 (c), all the peaks are superimposed from both PZT phase and NZFO phase. The result indicates the multilayered nanocomposite films can be obtained firing at 600℃ via the sol solutions modified

by the polymer-assistant PVP. Therefore, the preparation of PZT-NZFO multilayered nanocomposite is successful using the polymer-assisted sol-gel processing route.

Figure 3 shows the natural surface morphologies for the typical PZT-NZFO nanocomposite thin films firing at 600℃. As shown in Fig. 3(a), a high dense, uniform, and crack-free nanocomposites films are obtained, the average grain size in the surface NZFO layer is about 35nm and the roughness is about 80nm shown in Fig. 3(b).

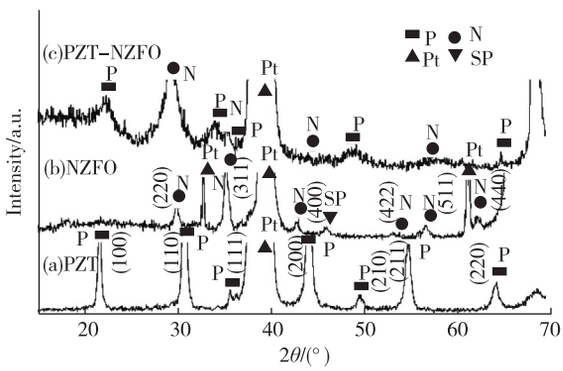

Fig. 2 The XRD patterns of PZT, NZFO and PZT/NZFO films , Note that P, N, Pt, and SP symbol PZT, NZFO, Pt-substrate and Stray-phase phase peaks, respectively

As shown in Figure 4, the well-controlled and uniform nanocomposite films with the thickness of 1200nm are observed. For PZT-NZFO nanocomposite thin films, the thickness of double PZT phase layers is about 300nm (i. e. each layer of about 150nm), and the thickness of one NZFO phase layer is about 110nm. Note that the thickness of one layer can be reproducible and controlled in a simple and easy way, which is one merit of the sol-gel precursors modified by the polymer-assistant. We contribute to the polymer-assistant PVP-K30 employed in the investigation, which enhances the adhesion of the PZT and NZFO films depositing on the substrate with an optimum viscosity of PZT and NZFO film sol precursor solutions, respectively.

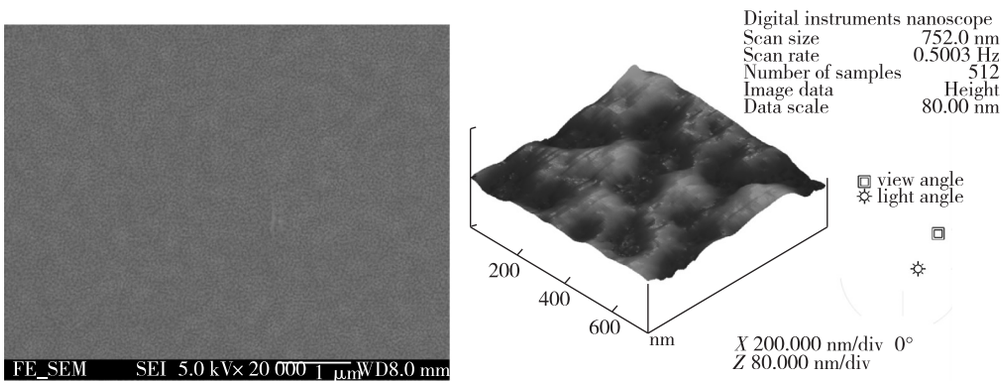

(a) The image of SEM (b) The image of AFM

Fig.3 The SEM and AFM images of the surface of PZT-NZFO films firing at 600 ℃

Figure 4 shows the cross-sectional backscattering electron (BSE) images for the nanocomposite films firing at 600℃. Because the average atomic number of PZT is larger than that of NZFO, therefore, in the BSE images the PZT layer appears lighter in color than the NZFO layer.

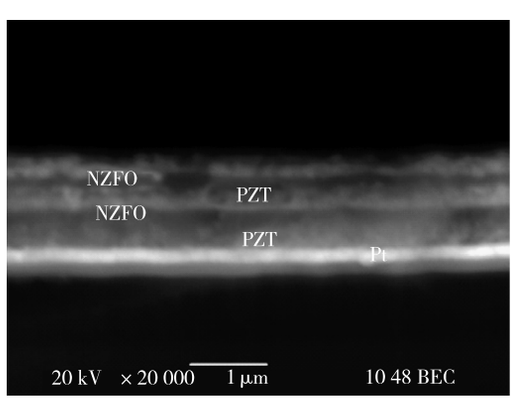

Fig.4 The cross-sectional backscattering electron images of PZT-NZFO film firing at 600℃

2.2 Magnetic properties

Figure 5 shows the magnetic-hysteresis loops of the pure NZFO film and multilayered nanocomposite films firing at (a) 500℃, and (b) 600℃ respectively, measured by applying magnetic fields parallel to the

film planes at room temperature.

Shown in Figure 5, all the film samples exhibit typical ferromagnetic hysteresis loops, indicating the presence of ordered magnetic structure in the films. It is obvious that the magnetization values (M_s) of the multilayered films are lower than the counterpart of the pure NZFO films due to the effect of the nonferromagnetic PZT layers, for example, for the pure NZFO film at 500℃, the M_s is 1.81×10^5 A/m, and 2.6×10^4 A/m for nanocomposite films respectively. While for the intrinsic coercivity (H_{ci}), 4.69×10^3 A/m for the pure NZFO film, and 1.19×10^4 A/m for PZT-NZFO films, which is attribute to the PZT grain size layer existing in the nanocomposite films. As compared with the pure NZFO, the magnetic properties of the PZT-NZFO nanocomposite thin films are decreased illustrating the effect of the layer thickness of PZT. In fact, as shown in Figure 5, it denotes that the firing temperature of 500－600℃ is high enough for the multilayered nanocomposites films to obtain good magnetic properties.

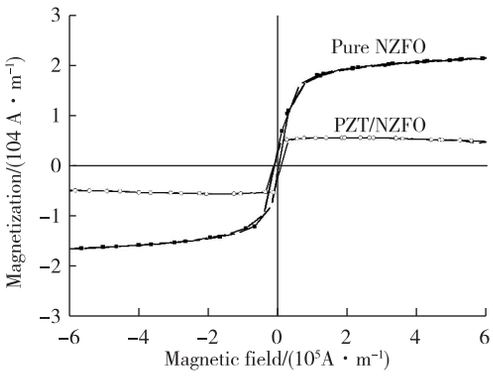

Fig. 5　Magnetic hysteresis loops of the pure NZFO films firing at 500℃ and the multilayered structured PZT-NZFO films at 600℃, respectively

2.3　Ferroelectric properties

Figure 6 shows the ferroelectric loops of these multilayered nanocomposite films, together with the pure PZT film firing at 600℃ at 1kHz and room temperature.

As shown in Figure 6, well developed ferroelectric loops are observed in the pure PZT and the nanocomposite films. For the PZT-NZFO thin films, the remnant polarization P_r and saturated polarization P_s are 15.7 and 20.95μC/cm^2, respectively. However, for the pure PZT film, the values of P_r and P_s are 24.02 and 35.4μC/cm^2, respectively. Because of the effect of the nonferroelectric NZFO layers, the polarization values for the nanocomposite films are relatively lower than those pure PZT derived by the same processing.

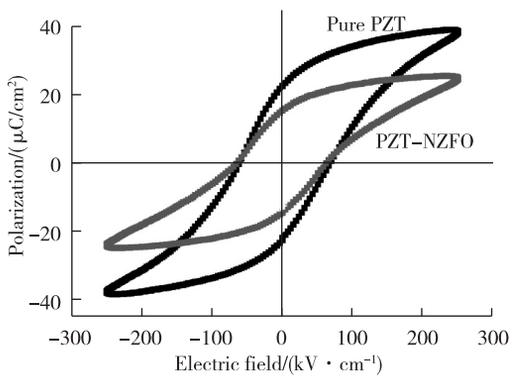

Fig.6　Polarization-electric field hysteresis loops of multilayered structured PZT-NZFO films, together with the pure PZT films firing at 600℃

2.4　Dielectric properties

Figure 7 shows the room-temperature dielectric properties as a function of frequency between 1kHz—10MHz for the multilayered PZT-NZFO nanocomposite film firied at 600℃, including the loss tangent shown in the inset, respectively. As shown in Figure 7.

In Figure 7, the dielectric constant decreases with the increase of the frequency, revealing with dielectric dispersion, at the same time, with increasing frequency, the loss tangent remains nearly constant

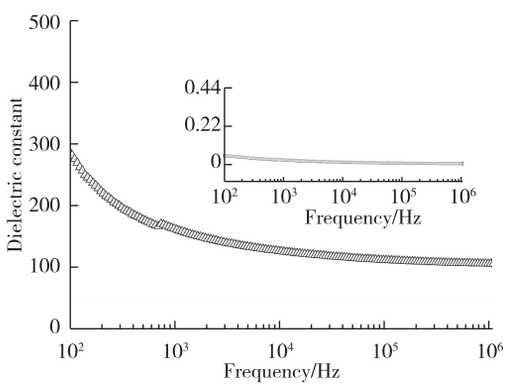

Fig.7　Frequency variation of dielectric constant of multilayered structured PZT-NZFO films, and the loss tangent in the inset firing at 600℃

value during the frequency range of 100Hz to 1MHz. The high dielectric constants measured at low frequencies might be attributed to the interfaces between the ferroelectric and ferromagnetic phases which have significantly different conductivities. These interfaces cause an additional polarization, the interfacial polarization, which boosts the dielectric constant and is in agreement with Koop's phenomenological theory[19]. And the constant value of loss tangent is assumed to be caused by the dipoles contributing to the polarization, indicating there is no diffusion phenomenon occurred in thin films firing at 600℃[20]. In Figure 7, at 1kHz and room temperature, the dielectric constant and loss tangent for the nanocomposite films are 165 and 0.02, respectively.

3 Conclusion

Multilayered PZT/NZFO nanocomposite films have been prepared successfully using the polymer-assistant PVP-K30 sol-gel route, and the crystallization of the films can be realized firing at 600℃ with a dense and well-controlled microstructure. Coexistence of ferroelectric and ferromagnetic properties at room temperature is confirmed by the P-E hysteresis loop and M-H hysteresis loop, respectively. Moreover, the appropriate dielectric constant with the low loss tangent at 1kHz and room temperature is obtained for the PZT/NZFO nanocomposite films fired at 600℃. More importantly, with the help of the PVP-K30, the phase composition of the multilayered structured multiferroic films can be easily controlled at nanoscale, offering a technical way to study the physical mechanism in nano-scale and potential applications in microelectronic devices.

参考文献:

[1]HILL N A. Why are there so few magnetic ferroelectrics [J]. The Journal of Physics Chemitry B, 2000, 104: 6694-6709.

[2]WANG K F, LIU J M, REN Z F. Multiferroicity: the coupling between magnetic and polarization orders[J]. Advances in Physics, 2009, 58: 321-448.

[3]SURYANARAYANA S V. Magnetoelectric interaction phenomena in materials[J]. Bulletin of Materials Science, 1994, 17:1259-1270.

[4]SUCH-TELEN J V. Product properties: a new application of composite materials[J]. Philips Research Reports, 1972, 27: 28-37.

[5]KANAI T, OHKOSHI S I, NAKAJIMA A, et al. A ferroelectric ferromagnet composed of $(PLZT)_x(BiFeO_3)_{1-x}$ solid solution[J]. Advance Material, 2001, 13: 487.

[6]GOTO T, KIMURA T, LAWES G, et al. Ferroelectricity and giant magnetocapacitance in perovskite rare-earth manganites[J]. Physics Review Letter, 2004, 92: 257201.

[7]LIU M, LI X, LOU J,et al. A modified sol-gel process for multiferroic nanocomposite films[J]. Journal of Applied Physics, 2007, 102: 083911.

[8]HE H C, WANG J, ZHOU J P, et al. Ferroelectric and ferromagnetic behavior of Pb $(Zr_{0.52}\ Ti_{0.48})O_3$-$Co_{0.9}Zn_{0.1}Fe_2O_4$ multilayered thin films prepared via solution processing[J]. Advance Function Material, 2007, 14: 1333-1338.

[9]HE H C, ZHOU J P, WANG J, et al. Multiferroic Pb$(Zr_{0.52}Ti_{0.48}O_3)$-$Co_{0.9}Zn_{0.1}Fe_2O_4$ bilayer thin films via a solution processing[J]. Applied Physics Letter, 2006, 89: 052904.

[10]WU H, XU B, LIU A P, et al. Strain-modulated magnetocapacitance of vertical ferroelectric-ferromagnetic nanocomposite heteroepitaxial films[J]. Journal of Physics D Applied Physics, 2015, 45(45): 455306.

[11]RAMESH R, SPALDIN N A. Multiferroics: progress and prospects in thin films[J]. Nature Materials,2007, 6: 21-29.

[12]NIE X L, LAN Z W, YU Z, et al. Microstructure and magnetic properties of nizn ferrite thin films prepared by sol-gel method[J]. Transactions of Nonferrous Metals Society of China,2007, 17: 854-857.

【下转第 17 页】

参考文献：

[1]LI K，GUO Y，MA F，et al. Design of ordered mesoporous H3 PW12 O40-titania materials and their photocatalytic activity to dye methyl orange degradation[J]. Catalysis Communications，2010，11：839-843.

[2]NOVOSELOV K S，GEIM A K，MOROZOV S V，et al. Electric field effect in atomically thin carbon films[J]. Science，2004，306(5696)：666-669.

[3]XU L，HUANG W Q，WANG L L，et al. Insights into enhanced visible-light photocatalytic hydrogen evolution of g-C_3N_4 and highly reduced grapheme oxide composite：the role of oxygen[J]. Chemistry of Materials，2015，27(5)：1612-1621.

[4]TIAN Y，LU H B，LIAO L，et al. Synthesis and evolution of hollow ZnO microspheres assisted by Zn powder precursor [J]. Solid State Communications，2009，149：456-460.

[5]周卫，张开富，潘凯，等. 高热稳定性多孔二氧化钛/石墨烯复合体的制备与光催化性能研究[J]. 中国科技论文，2014，9(12)：1414-1417.

[6]RAO C N R，BISWASK K，SUBRAHMANYAM K S，et al. Graphebe，the new nanocarbon[J]. Journal of Materials Chemistry，2009，19(17)：2457-2469.

[7]FENG M，SUN R Q，ZHAN H B，et al. Lossless synthesis of grapheme nanosheets decorated with tiny cadmium sulfide quantum dots with excellent nonlinear optical properties[J]. Nanotechnology，2010，21(7)：075601.

[8]郭书鹏. 石墨烯表面增强拉曼散射效应的探究[D]. 哈尔滨：哈尔滨工业大学，2013.

[9]安丽萍，刘念华. 具有边缘缺陷石墨烯纳米结的自旋输运特性[J]. 新型炭材料，2012，27(3)：181-187.

[10]李彪，徐大海，曾晖. 边缘重构对锯齿型石墨烯纳米带电子输运的影响[J]. 物理学报，2014(11)：250-255.

[11]范厚刚. 石墨烯/ZnO 复合材料光催化降解亚甲基蓝性能研究[D]. 四平：吉林师范大学，2015.

（责任编辑：李艳）

【上接第 12 页】

[13]TESTINO V，TRESILETTI P，NANNI A S. $BaTiO_3$-($Ni_{0.5}Zn_{0.5}$)Fe_2O_4 ceramic composites with ferroelectric and magnetic properties[J]. Journal of European Ceramic Society，2007，27：4379-4382.

[14]MITOSERIU L，PALLECCHI I，BUSCAGLIA V，et al. Magnetic properties of the $BaTiO_3$-(Ni，Zn)Fe_2O_4 multiferroic composites[J]. Journal of Magnetism and Magnetic Materials，2007，316：603-606.

[15]ZHANG H F，ZHANG L Y，YAO X. Fabrication and electrical properties of barium strontium titanate thick films by modified sol-gel method[J]. Journal of Electroceramics，2008，21(1)：503-507.

[16]ZHANG H F，YAO X，ZHANG L Y. Microstructure and dielectric properties of barium strontium titanate thick films and ceramics with a concrete-like structure[J]. Journal of Americal Ceramics Society，2007，90：2333-2339.

[17]KOZUKA H，KAJIMURA M. Single-step dip coating of crack-free $BaTiO_3$ films $>1\mu m$ thick：effect of poly(vinylpyrrolidone) on critical thickness[J]. Journal of the American Ceramic Society，2000，83：1056-1062.

[18]ROGACHEV A S，MUKASYAN A S. Combustion of heterogeneous nanostructural systems (review) [J]. Combustion，Explosion and Shock Waves，2010，46：243-266.

[19]KOOPS C G. On the dispersion of resistivity and dielectric constant of some semiconductors at audiofrequencies[J]. Physical Review Letters，1951，83：121-124.

[20]ZHANG H F，OR S W，CHAN H L W. Electrical，magnetic and magnetoelectric characterization of fine-grained Pb($Zr_{0.53}Ti_{0.47}$)O_3-($Ni_{0.5}Zn_{0.5}$)Fe_2O_4 composite ceramics[J]. Journal of Alloys and Compounds，2011，509：6311-6316.

（责任编辑：李艳）